Self-healing and wide temperature tolerant flexible supercapacitor based on ternary-network organo-hydrogel electrolyte

Hengyu Zheng[1], XiaoJun Du[1], Qingxiao Liu[1], KangTai Ou[1], Yang Cao[1], Xin Fang[1], Qiang Fu[1, 2], Youyi Sun[1*]

[1] School of materials science and technology, North University of China, Taiyuan 030051, P.R. China.

[2] School of Civil and Environmental Engineering, University of Technology Sydney, Ultimo NSW 2007, Australia..

Abstract: A novel ternary network organo-hydrogel electrolyte is developed to improve the environmental adaptability of flexible supercapacitors. The ternary network electrolyte is composed of graphene/boric acid/polyvinyl alcohol matrix and methyl sulfoxide/water/H_2SO_4 mixture. A flexible supercapacitor with a sandwich structure is further assembled with the electrolyte and two polyaniline fiber/carbon cloth electrodes. The supercapacitor exhibits a high capacitance retention rate (90%) after 5 cuting/self-healing cycles. Furthermore, supercapacitors have high specific capacitance and capacitance retention on a wide temperature range of -65°C to 65°C. The specific capacitance of supercapacitor is about 237.8 F/g and 152 F/g at 65℃ and -65℃, in which the corresponding capacitance retention of supercapacitor is about 110.5% and 70.7%, respectively. The work provides an effective strategy to design and prepare flexible electrolyte with broad temperature adaptability, good self-healing ability and good mechanical flexibility for flexible energy storage devices.

Keywords: organo-hydrogel, graphene, wide temperature, supercapacitors, self-healing.

Responding author: Fax: 86-351-3922949

E-mail address: syyi@pku.edu.cn (YY Sun).

1.Introduction

Flexible supercapacitor has attracted lots of attentions due to the fast charge-discharge speed, light weight, good flexibility, portability and highly power density for application in flexible/wearable electronic devices[1-3]. In some instances, flexible supercapacitors need to work in harsh environments (eg. severe cold and hot regions) or to automatically restore its electrochemical performance in the event of physical damage (eg. cutting or breaking)[4, 5]. Therefore, the wide temperature-tolerant and self-healing flexible supercapacitors is highly desired for special application in flexible/wearable electronic devices. As well-known, these performances of a flexible supercapacitor strongly depend on the structure and properties of its electrolyte[6-8]. So, lots of gel electrolytes were prepared and developed for application in wide temperature-tolerant and self-healing flexible supercapacitors[9-18]. For example, cross-linked poly(vinyl alcohol)/montmorillonite/$Zn(ClO_4)_2$ gel electrolyte was synthesized for application in flexible supercapacitor with a temperature range from -50℃ to 80℃[15]. A novel choline chloride/ethylene glycol/urea ternary gel electrolyte was synthesized for application in flexible supercapacitor with a temperature range from -40℃ to 115℃[18]. A novel PVdF-HFP/EMITf/$Al(Tf)_3$ gel electrolyte membrane was prepared for application in flexible supercapacitor with a temperature of -20℃ to 60℃[10]. The tetraethylammonium tetrafluoroborate/propylene carbonate (Et_4NBF_4/PC) gel electrolyte was prepared for application in flexible supercapacitor with a temperature of -20℃ to 50℃[17]. A novel polyacrylamide/montmorillonite/ionic liquid-Li_2SO_4 hydrogel electrolyte was prepared for application in flexible supercapacitor with a temperature of -10℃ to 80℃[9]. A novel CS-PAAm hydrogel electrolyte was prepared for application in flexible supercapacitor with a temperature of -60℃ to 100℃[14]. A montmorillonite flake/polyvinyl alcohol organic-hydrogel electrolyte was prepared for application in flexible supercapacitors with a temperature of -40℃ to 80℃[11]. A montmorillonite/poly(vinyl alcohol) (MMT/PVA/H_2SO_4 DMSO/H_2O) organo-hydrogel electrolyte was prepared for application in flexible supercapacitor with a temperature of -50℃ to 90℃[13]. A anionic carrageenan gels/poly(vinyl alcohol) ethylene glycol hydrogel electrolyte was prepared for application in flexible supercapacitor with a temperature of -40℃ to 60℃[16]. P($AMPS_{0.3}$-co-$AAM_{0.4}$)/DMSO/LiCl/H_2O organic-hydrogel was prepared for application in flexible supercapacitor with a temperature of -20℃ to 100℃[12]. From above respects, although there are lots of works reporting flexible supercapacitor with a wide operating

temperature, yet, these flexible supercapacitors do not possess self-healing performance. Genrally, it needs dynamic and physical bonds in organo-hydrogel electrolyte for self-healing properties. However, the conventional organo-hydrogel electrolytes with self-healing properties show poor thermal and mechanical stability due to the easy break of dynamic and physical bonds at high temperature. Therefore, up to now, it is still a high challenge to prepare flexible supercapacitors with simultaneously wide temperature tolerant and self-healing performance.

Based on above consideration, a new ternary-network organo-hydrogel electrolyte is developed to improve temperature tolerant and self-healing performance of conventional flexible supercapacitors. The PVA chains with various alcoholysis degrees form a ternary-network under assistance of graphene and boric acid, providing the self-healing properties and thermal stability. The DMSO and H_2SO_4 are also introduced to provide good ionic conductivity at wide temperature. Therefore, the composite organo-hydrogel electrolyte does not only exhibit good electrochemical performance at a wide temperature, but also possesses high self-healing property

2.Experimental

2.1 Material

Polyvinyl alcohol (PVA 1788 and 1799) was purchased from Hefei Qiansheng Biotechnology Co., Ltd. Dimethyl sulfoxide (DMSO) and boric acid (BA) were purchased from Tianjin Damao Chemical Co., LTD. Carbon cloth was purchased from Taiwan carbon energy company. Aniline ($C_6H_5NH_2$) was purchased from Tianjin Damao chemical reagent factory. H_2SO_4 was purchased from McLean Reagent Co., Ltd. The graphene was prepared by ourselves.

2.2 Preparation of self-healing and wide temperature tolerant organo-hydrogel electrolyte

The organo-hydrogel electrolyte was prepared by a frozen-thawed method as shown in following. 6g DMSO and 4g water were mixed to form mixing solvent. 0.06g graphene was dispersed in above mixing solvent under ultrasonic. The 1.5g PVA (weight ratio of PVA1788/1799=4/1) was dissolved to the above solution at 97℃, forming PVA/graphene/DMSO/H_2O sol. The mixing sol was frozen at -15℃ for 1.0h, and then thawed at room temperature for 12h to form PVA/graphene/DMSO/H_2O organo-hydrogels. Finally, the organo-hydrogel was immersed in 0.1M boric acid solution for 6h and then transferred to 2M sulfuric acid solution for 12h, forming self-

healing PVA/graphene/DMSO/BA/H_2SO_4 composite organo-hydrogel electrolyte with high conductivity.

2.3 Preparation of polyaniline (PANI)/carbon cloth (CC) electrode

The PANI/CC electrode was prepared by electrochemical deposition method according to previous work[19]. The electrochemical deposition process was carried out in aqueous solution containing 0.2M aniline monomer and 0.5M H_2SO_4 by three electrode system. The carbon cloth, saturated calomel electrode and platinum sheet electrode acted as working electrode, reference electrode and counter electrode, respectively. The PANI materials were deposited on surface of carbon cloth by cyclic voltammetry at a scanning rate of 0.1V/s at a voltage of -0.1V to 0.8V for 90 times. The obtained PANI/CC was washed for several times with deionized water, and then dried at room temperature. The loading mass of PANI in PANI/CC was about 1.04 mg/cm^2.

2.4 Fabrication of flexible supercapacitors

A flexible supercapacitor with sandwich structure was fabricated from organo-hydrogel electrolyte and PANI/CC electrodes by self-assembly method as shown in following. Firstly, the PVA/graphene/DMSO/H_2O sol was coated on the surface of PANI/CC electrode (0.8cm×1.5cm×0.5cm), and the other PANI/CC electrode was covered on it, forming a sandwich flexible film. The sandwich flexible film was frozen at -15℃ in refrigerator for 1.0h and then thaw it room temperature for 12h, forming a sandwich flexible film based on organo-hydrogel. The sandwich flexible film was further immersed in 0.1M boric acid solution for 6h and then transferred to 2M sulfuric acid solution for 12h, forming flexible supercapacitor.

2.5 Characterization

The micro-structure of organo-hydrogel was characterized by scanning electron microscopy (SEM) (Phenom-XL). The organo-hydrogel was swelled in deionized water to remove organic solvents, forming hydrogel. The hydrogel was then frozen rapidly in liquid nitrogen and then transferred to a freeze dryer for cold dry 12h.

The crystal structure of organo-hydrogel was characterized by X-ray diffractometer (DX-2700B). The XRD data was collected with Cu Kα radiation at 40 kV at an angle of 2θ=5~80°.

The Fourier transform infrared specrtra of organo-hydrogel was characterized in the range of 500-4000cm^{-1} by the ATR test in the Fourier transform infrared (FT-IR) spectrometer (Thermo Nicolet 360) The preparation of testing sample was same with SEM testing.

The Raman spectroscopy of organo-hydrogel was characterized by a LabRAM HR-800 Raman spectrometer with an incident laser beam of 532.4nm (Horiba Scientific), objective 20, excitation power ⩾170mW.

The electrical conductivity (σ, S/cm) of the organo-hydrogel was obtained by electrochemical workstation (MS310, Wuhan, China) according to the following equation (1)[20, 21].

$$\sigma = L/AR \qquad (1)$$

Where, L is the thickness of the organo-hydrogel, R is the equivalent series resistance, A represents the contact area of the organo-hydrogel with carbon cloth.

Self-healing perproties of organo-hydrogel was characterized as shown in following. The organo-hydrogel was firstly cut by scissors and then connected for 5min. The process was recorded by camera.

2.6 Electrochemical performance

The electrochemical performance of flexible supercapacitors was characterized by electrochemical workstation (MS310, Wuhan, China). The galvanostatic charge-discharge (GCD) curves were obtained at the different current densities within a voltage window of -0.7 to 0.7V. The cyclic voltammetry (CV) curves were obtained from -0.7 to 0.7V at the different scanning rates. The EIS was obtained from 100kHz to 0.01Hz with an amplitude of 5.0mV at an open-circuit voltage.

The specific capacitance (C_m, F/g), energy density (E_{cell}, Wh/kg), power density (P_{cell}, W/kg) and Coulombic efficiency of the supercapacitors were calculated from GCD curves according to the equation 2, 3, 4 and 5, respectively[22-24].

$$C_m = \frac{I \cdot \Delta t}{m \cdot \Delta V} \qquad (2)$$

$$E_{cell} = \frac{Cm \times (\Delta V)^2}{2 \times 3.6} \qquad (3)$$

$$P_{cell} = \frac{E_{cell} \times 3600}{\Delta t} \qquad (4)$$

$$\text{Coulombic efficiency } (\%) = \frac{\text{discharge time}}{\text{charge time}} \times 100\% \qquad (5)$$

Where $m(mg)$, ΔV (V), I(A) and Δt(s) are the total mass of active materials in the two electrodes, the working potential window, the discharge current and discharge time, respectively.

Self-healing performance of supercapacitor was also characterized as shown in following. The flexible supercapacitor was cut off and then was connected at room temperature. In addition, the conductive silver paste was filled into crack of the cut

carbon cloth. After self-healing, the electrochemical performance of cut supercapacitor was further characterized. The cut/self-healing process was repetitiveely carried out on same place of a supercapacitor. And the ectrochemical performance of was investigated as a fucntion of cut/self-healing cycles.

The electrochemical performance of supercapacitor was also characterized as a function of temperature in water bath or low temperature reaction bath (DFY-5/80).

3.Result and Discussion

Here, a new graphene/BA/PVA organo-hydrogel with high ionic conductivity, good thermal stability and good self-healing capability was developed, which was composed of PVA, graphene, H_2O, DMSO, BA and H_2SO_4 (Fig.1A). The DMSO/H_2O mixture was employed to improve the anti-freezing property of the organo-hydrogel. It was attributed to the strong hydrogen bonding between DMSO and H_2O molecules, effectively reducing the freezing point and enhancing the boiling point of water[25]. The H_2SO_4 was further introduced to organo-hydrogel electrolyte, enhancing the ionic conductivity[26, 27]. The formation of present organo-hydrogel was mainly attributed to hydrogen bonding between -OH groups of PVA chains, forming first physical cross-linking network. Here, the chemical structure of PVA palyed important role for obtaining high-temperature stability of present organo-hydrogel. The organo-hydrogel or hydrogel could be easily prepared by combing PVA1788 with freeze-thaw process[28]. However, these PVA1788 based organo-hydrogel or hydrogel showed poor thermal stability, in which the PVA1788 based organo-hydrogel or hydrogel easily transfered to sol or liquid at higher temperature than 40℃ (in Fig.1B-a). The problem restricted the application of PVA1788 based organo-hydrogel or hydrogel in flexible supercapacitor with high temperature. The result was due to relatively low alcoholysis degree of PVA1788, leading to a relatively low physical cross-linking density. So, here, the PVA1799 with high alcoholysis degree was also added to organo-hydrogel, enhancing physical cross-linking density (Fig.1A). However, the PVA1799 was difficult to dissolve in DMSO/H_2O mixture (in Fig.1C). In addition, PVA1799 based hydrogel showed poor self-healing properties due to form lots of intermolecular hydrogen bondings. Therefore, the PVA1788/PVA1799 (weight ratio of 4:1) mixture was used to improve thermal stability (in Fig.1B-b). The boric acid was also introduced to organo-hydrogel to obtain good self-healing properties. The good self-healing properties were mainly attributed to formation of boronic ester bonds between the PVA chain and boric acid, building a second dynamic cross-linked network. Contrarily, it was difficult to

obtain self-healing properties for the organo-hydrogel without boric acid (in Fig.1D). The graphene was also introduced to organo-hydrogel, forming third physical cross-linked network by intermolecular hydrogen bonding between PVA and graphene. It did not only enhance the mechanical stability, but also reduced the diffusion resistance and intrinsic resistance of organo-hydrogel. The construction of this novel ternary cross-linked network did not only endow the organo-hydrogel with excellent wide temperature tolerant stability, but also endowed the organo-hydrogel with good self-healing properties.

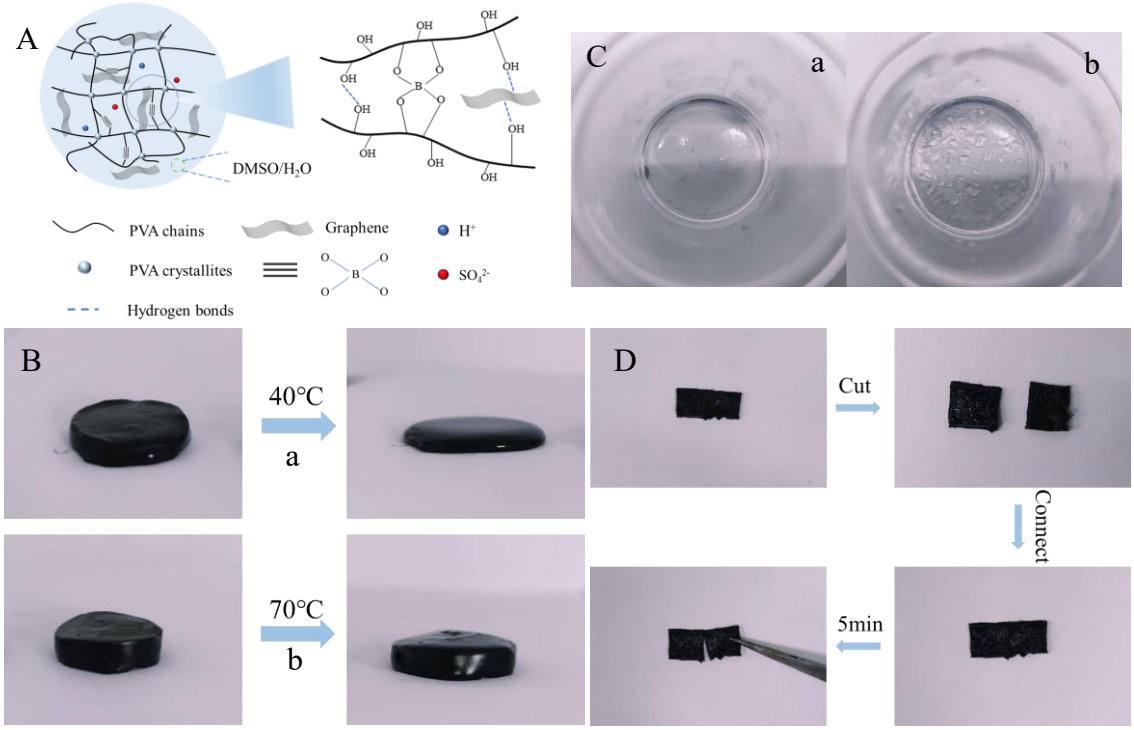

Fig.1. (A)Schematic diagram in structure of the graphene/BA/PVA organo-hydrogel, (B)Optical images of (a) PVA (1788) organo-hydrogel and (b) hybrid PVA (1788/1799) organo-hydrogel at high temperature, (C) Optical images of (a) 0.3g PVA1799 and (b) >0.3g PVA1799 dissolved in DMSO/H_2O solution, (D) Optical images of graphene/PVA organo-hydrogel electrolyte after cutting and connecting.

The formation of graphene/BA/PVA organo-hydrogels was confirmed by the FT-IR, Raman and XRD spectra. As shown in the FT-IR spectra (Fig.2A), the two absorption peaks at 3382cm^{-1} and 2918cm^{-1} were assigned to O-H stretching and C-H stretching vibrations of PVA, respectively[29]. The absorption peaks at 1026 cm^{-1} and 1124 cm^{-1} were assigned to the symmetric and asymmetric stretching vibrations of S=O groups of DMSO and H_2SO_4, respectively[12]. These absorption peaks were also observed in graphene/BA/PVA organo-hydrogels. In a comparison, the absorption peak

assigned to -OH was red shift after addition of graphene nanosheets, indicating the formation of hydrogen bonding between graphene and PVA. Furthermore, a new peak was observed at 1340cm^{-1}, which was assinged to the characteristic absorption of boronic ester (B-O) bonds[30]. The weak characteristic absorption of boronic ester was due to its low content. These results confirmed the presence of DMSO, H_2SO_4, BA and PVA in organo-hydrogels, in which the hydrogen bonding between PVA and boric acid or graphene was formed. Fig.2B shows the Raman spectra of graphene/BA/PVA organo-hydrogels and the results were conclued in Table 1. The two absorption peaks at 2920cm^{-1} and 1419cm^{-1} were clearly observed, which were assigned to stretching vibrations of -CH_2 and -CH of PVA, respectively[28, 31]. In addition, there were two new absorption peaks at 1357cm^{-1} and 1597cm^{-1}, which were assigned to characteristic D and G bands of graphene[28, 29]. The result indicated the presence of graphene in organo-hydrogels. Fig.2C shows the XRD spectra of BA/PVA organo-hydrogel and graphene/BA/PVA organo-hydrogel. The two organo-hydrogels both showed a strong peak at $2\theta=19.7^{o}$, which was assigned to PVA crystallization. The micro-structure of PVA organo-hydrogel was also characterized by SEM images. As shown in Fig.2D, the PVA organo-hydrogel exhibited a relatively compacted structure and few pores comparing to conventional PVA hydrogels[32]. This result was attributed to the shrink of PVA network in the process of solvent exchange. In contrast, the BA/PVA organo-hydrogel had more porous structures (Fig.2E). This was due to further cross-linking between PVA and boric acid, restrcting the shrink of PVA network. At the same reason, the addition of graphene (Fig.2F) further enriched the porous structure of the organo-hydrogel, which was due to the formation of a hydrogen bond cross-linking network between graphene nanosheets and PVA.

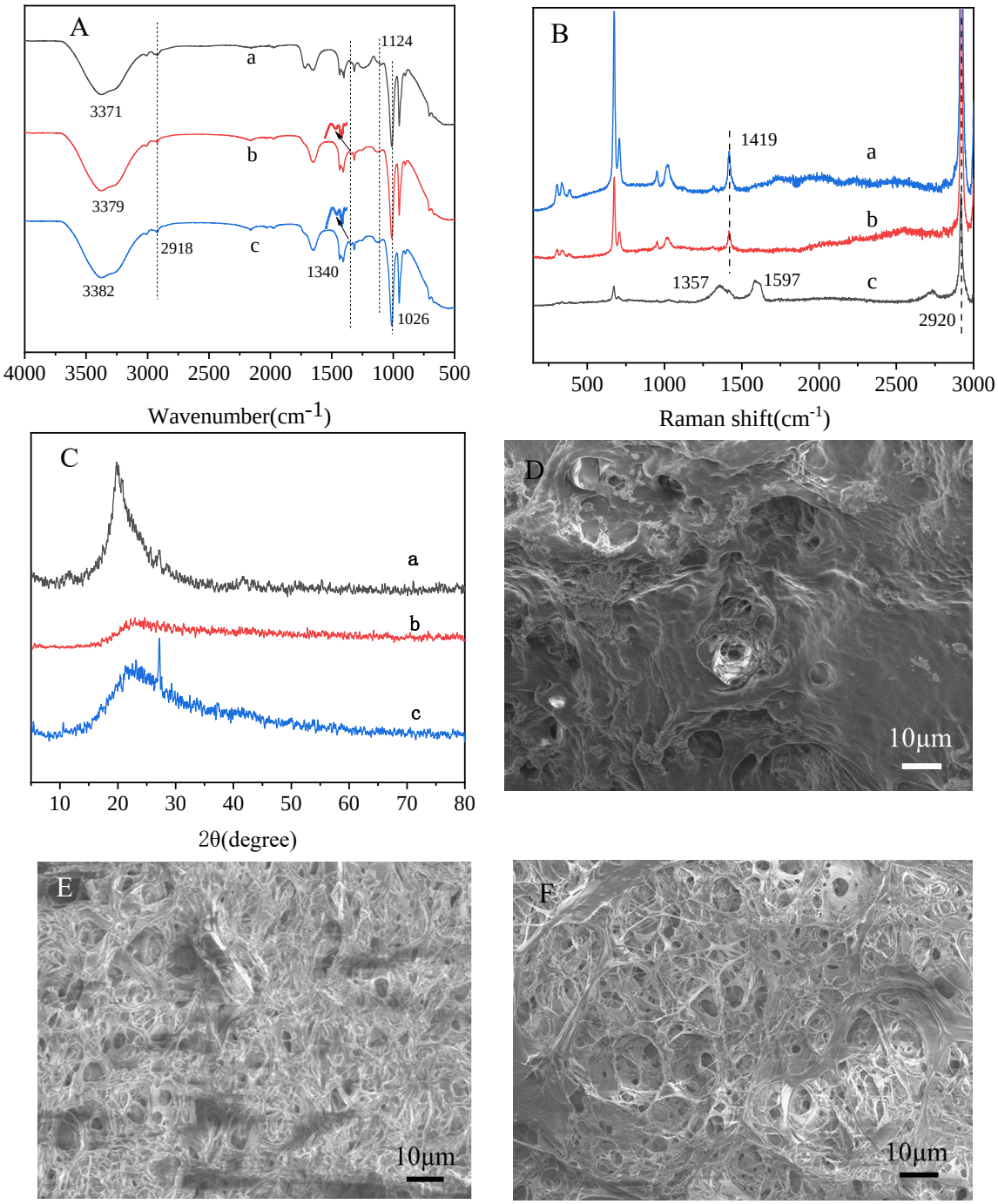

Fig.2. (A) FTIR spectra, (B) Raman spectra and (C) XRD patterns of (a) PVA organo-hydrogels, (b) BA/PVA organo-hydrogels and (c) graphene/BA/PVA organo-hydrogels. Cross section SEM images of (D) PVA organo-hydrogel, (E) BA/PVA organo-hydrogel and (F) graphene/BA/PVA after removing DMSO and freeze drying.

Table.1. The result of FT-IR and Raman spectra of the hydrogels after drying.

Measurement	Wavelength(cm^{-1})	Band characteristics	Reference
FT-IR	1026	S=O symmetric tensile vibration	[12]
	1124	S=O Asymmetrical tensile vibration	[12]
	1340	B-O telescopic vibration	[30]
Raman	2920	CH_2 tensile vibration	[31]
	1419	C-H tensile vibration	[28]
	1357	D-band of graphene	[28]
	1597	G-band of graphene	[28]

The mechanical properties of graphene/BA/PVA organo-hydrogels and hydrogel were characterized and compared as shown in Fig.3. The organo-hydrogels and hydrogel could be both stretched at room temperature, indicating a good flexibility and mechanical stability (Fig.3A). However, the graphene/BA/PVA hydrogel became brittleness and was easily broke under bending force at -25ºC (in Fig.3A-b). Contrarily, the graphene/BA/PVA organo-hydrogel still exhibited good flexibility at ultra-low temperature of -65℃, in which it could be easily bent for 180º (in Fig.3A-a). The result confirmed the excellent anti-freeze performance of present graphene/BA/PVA organo-hydrogel. In addition, the organo-hydrogels showed a high ionic conductivity (*ca.* 4.0S/m) at 65℃ (Fig.3B). As expected, the ionic conductivity of organo-hydrogels decreased with decreasing in temperature. The result was due to the decrease of dissociation and ion diffusion at low temperature. However, it still showed a relatively high ionic conductivity of ca. 0.7S/m even at -65℃, which was difficult to be observed in the previous works[13, 33-38]. The result was attributed to the high solubility and rapid mobility of H^+ and SO_4^{2+} in DMSO/water mixture[38]. Fig.3C shows the optical photos of LED light by the conducting wire based on graphene/BA/PVA organo-hydrogel as a function of temperature. All LED lights could be lighted up at subzero temperatures, even at -65℃. The result further confirms high ionic conductivity of graphene/BA/PVA organo-hydrogel in a wide temperature range from -65℃ to 65℃.

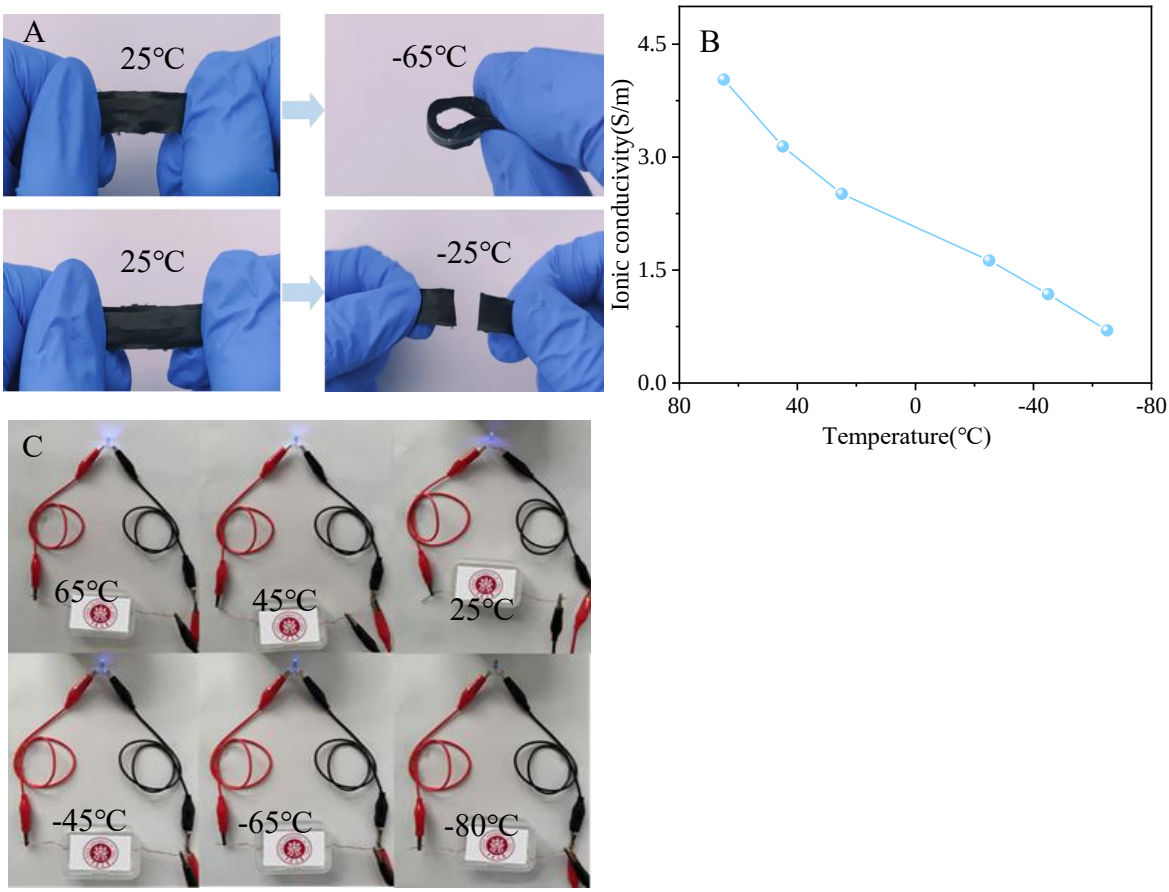

Fig.3. (A) Optical photos of (a) graphene/BA/PVA organo-hydrogel and (b) graphene/BA/PVA hydrogel under various forces and temperatures. (B) Ionic conductivity of graphene/BA/PVA organo-hydrogel as a function of temperature. (C) Optical photos of LED light by using a graphene/BA/PVA organo-hydrogel conductor under various temperatures.

The self-healing properties of graphene/BA/PVA organo-hydrogel were evaluated as shown in Fig.4. A graphene/BA/PVA organo-hydrogel was firstly tailor into two symmetrical pieces and then put them tightly together (Fig.4A). It was found that the two originally separated parts were naturally bonded to form a new whole after a 10s, and it showed good mechanical stability after 5min. In a comparison, the two originally separated parts were not naturally bonded to form a new whole and there were large cracks for the graphene/PVA organo-hydrogel after 5min (Fig.1D). The cutting/healing process of graphene/BA/PVA organo-hydrogel was further confirmed by the optical microscope (in Fig.4B). It was no obvious gap in the healing area. These results indicated that the addition of BA played important role for the self-healing properties. The good self-healing properties of graphene/BA/PVA organo-hydrogels were attributed to the formation of borate ester between BA and PVA[29, 39]. The effect of

temperature on self-healing properties of graphene/BA/PVA organo-hydrogel was also investigated as shown in Fig.4C. The graphene/BA/PVA organo-hydrogel could be self-healing at a wide temperature from -65℃ to 65℃. The phenomenon was difficult to be observed in hydrogels[40-45] . Fig.4D shows the optical photos of LED light by the conducting wire based on graphene/BA/PVA organo-hydrogel after the cutting and self-healing. The LED was not lighted up by graphene/BA/PVA organo-hydrogel after cutting, and then the LED could be lighted up after self-healing. The result further confirmed the excellent self-healing properties of graphene/BA/PVA organo-hydrogel

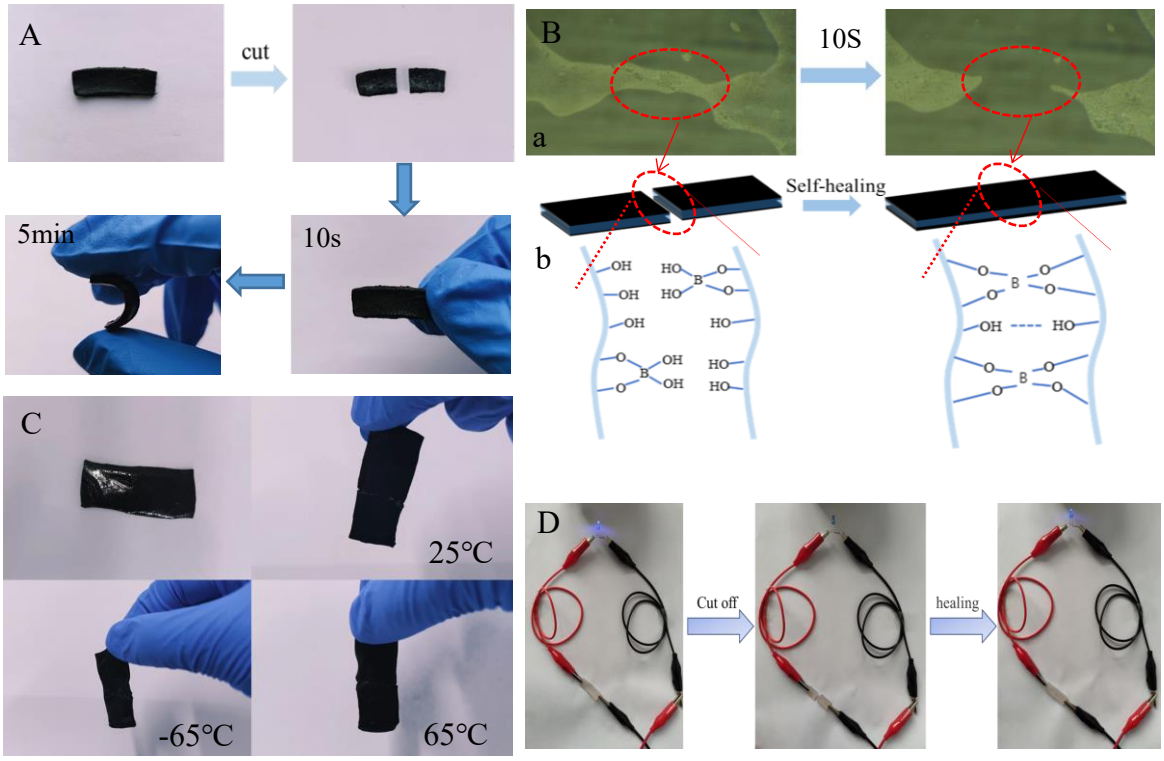

Fig.4. (A) Optical images of the self-healing process for graphene/BA/PVA organo-hydrogel at room temperature. (B) (a)Optical microscope images of electrolytes with different self-healing times, (b) Schematic diagram of the self-healing mechanism of graphene/BA/PVA organo-hydrogel. (C) Optical photos of self-healing process of graphene/BA/PVA organo-hydrogel at different temperatures. (D) Optical images of blue LED lit after cutting and self-healing of graphene/BA/PVA organo-hydrogel.

A flexible sandwich supercapacitor was designed and fabricated from organo-hydrogel electrolyte and PANI/CC electrodes. The CV curves of the supercapacitors based on various organo-hydrogel electrolytes were characterized and compared at a scanning rate of 100mV/s as shown in Fig.5A. The two supercapacitors both showed rectangular and symmetrical CV curves, indicating good capacitive performance. The

supercapacitor based on graphene/BA/PVA organo-hydrogel showed larger CV areas, indicating a larger specific capacitance comparing to BA/PVA organo-hydrogel. The result was attributed to the rapider ionic and electron transport of graphene/BA/PVA organo-hydrogel comparing to the BA/PVA organo-hydrogel. The charge-discharge (GCD) curves of two supercapacitors were also characterized and compared at 0.4 A/g as shown in Fig.5B. The GCD curves both showed symmetrical and triangular shape, indicating a typical double-layer character[29]. The discharge time of supercapacitor based on graphene/BA/PVA organo-hydrogel was larger, indicating a larger special capacitance. The special capacitance of supercapacitors based on graphene/BA/PVA and BA/PVA organo-hydrogel was about 265.2 F/g and 235.1 F/g at 0.4 A/g, respectively. The EIS spectra of two supercapacitors were also characterized and compared as shown in Fig.5C. The two EIS curves both exhibited a straight line with large slope in the low frequency region, indicating a low ion diffusion resistance[12]. According to the analog equivalent circuit in the illustration (inset of Fig.5D), where equivalent series resistance (Rs) is the resistance of the organic hydrogel electrolyte and charge-transfer resistance (Rct) is the charge transfer resistance at the interface between the electrolyte and the electrode. The graphene/BA/PVA organo-hydrogel showed smaller Rs (ca. 3.1Ω) comparing to BA/PVA organo-hydrogel (ca. 5.4Ω). This result was attributed the lower resistance of electron and ionic transport in graphene/BA/PVA organo-hydrogel, leading to a smaller internal resistance. Furthermore, there was almost no semicircle in the high frequency region, indicating a low Rct. Among them, the Rct of BA/PVA and Graphene/BA/PVA organic hydrogel supercapacitors was about 5.7 and 3.5Ω, respectively. It was seen that after the addition of graphene, the Rct between the electrolyte and the electrode of the supercapacitor decreased. This showed that the contact between the electrode and the electrolyte of the graphene/BA/PVA organic hydrogel-based supercapacitor was better, and the diffusion resistance between the electrode and the electrolyte was lower, thereby enhancing the capacitance behavior[46, 47]. These results coincide with CV and GCD test results.

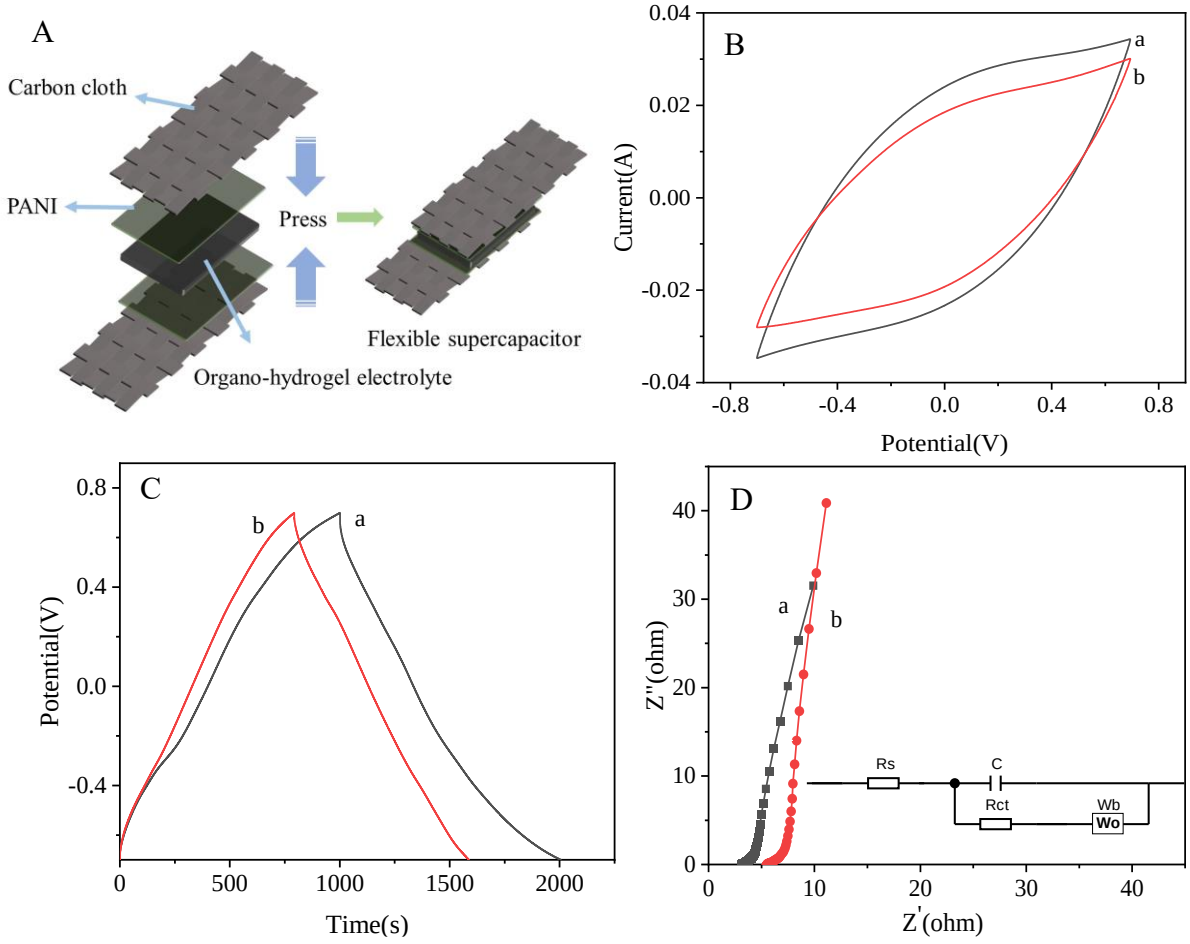

Fig.5. (A) Structural schematic diagram of flexible supercapacitor. (B) CV curves, (C) GCD curves and (D) EIS spectra of supercapacitors based on (a) graphene/BA/PVA organo-hydrogel and (b) BA/PVA organo-hydrogel electrolyte. The inset of Fig.5D is equivalent circuit model of present supercapacitor.

The electrochemical performance of supercapacitor based on graphene/BA/PVA organo-hydrogel was further investigated as a function of temperature. All CV curves showed rectangular and symmetrical CV curves, indicating good capacitive performance at a wide temperature range from -65℃ to 65℃ (in Fig.6A). In addition, the area of CV curves obviously decreased with deceasing in temperature, indicating a lower capacity at lower temperature. Above result was further confirmed by the GCD curves as a function of temperature as shown in Fig.6B. The discharge time of the supercapacitor clearly decreased with deceasing in temperature, further indicating a lower capacity at lower temperature. The specific capacitance of supercapacitor was about 237.8 F/g, 216.8 F/g, 215 F/g, 177.5 F/g, 173.9 F/g and 152 F/g at 65℃, 45℃, 25℃, -25℃, -45℃ and -65℃, respectively (Fig.6C). The capacitance retention of supercapacitor was about 110.5% and 70.7% at 65℃ and -65℃ comparing to the result

at 25℃, respectively. The different capacitance retention of present supercapacitor was attributed to that resistance of ion diffusion decreased with decreasing in temperature. The result also strongly confirmed the wide temperature tolerant performance for the present flexible supercapacitor.

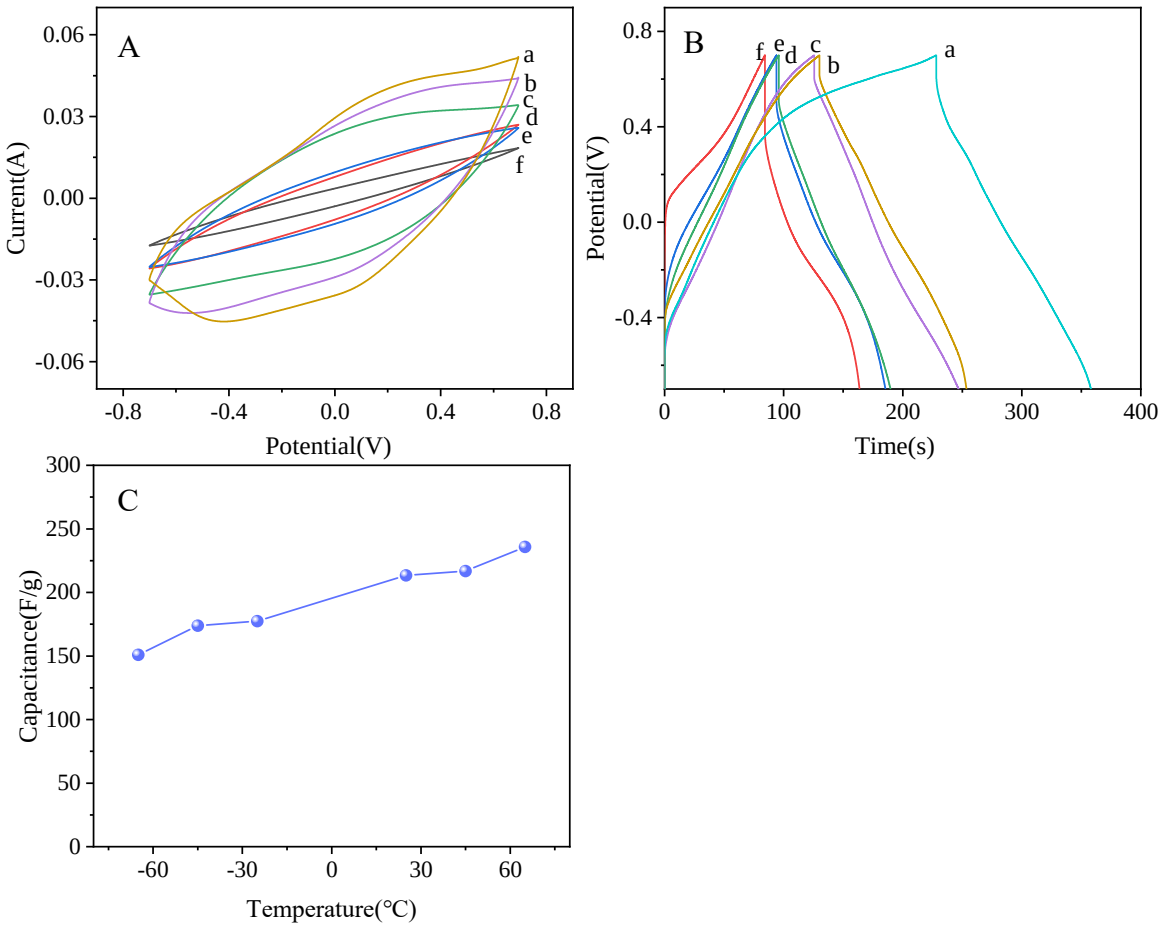

Fig.6. (A)CV curves and (B) GCD curves of the supercapacitor based on graphene/BA/PVA organo-hydrogel electrolyte at various temperatures of (a) 65℃, (b) 45℃, (c)25℃, (d)-25℃, (e)-45℃ and (f)-65℃. (C) Specific capacitance of supercapacitor based on graphene/BA/PVA organo-hydrogel electrolyte at 2.0A/g as a function of temperature.

The self-healing performance of supercapacitor based on graphene/BA/PVA organo-hydrogel was further evaluated as a function of cutting/self-healing cycles. Here, it should be noted that the cut PANI/CC electrode was repaired by filling with conductive silver paste[26]. Fig.7A shows the CV curves of supercapacitor at 100 mV/s as a function of cutting/self-healing cycles. All supercapacitors showed similar CV curves, which were still few changes even after 5 cutting/self-healing cycles. The similar phenomenon was also observed in GCD curves of supercapacitors at 2.0 A/g

(Fig.7B). The specific capacitance of supercapacitor was about 215F/g, 208.6F/g, 206.6F/g, 203.8F/g, 200.5F/g and 193 F/g under 0, 1th, 2th, 3th, 4th and 5th cutting/self-healing, respectively (Fig.7C). The capacitance retention of supercapacitor was about 90% after 5 cutting/self-healing cycles (Fig.7C). The good self-healing performance of supercapacitor was further confirmed by the EIS spectra as shown in Fig.7D. It clearly showed a similar EIS curve and equivalent circuit for supercapacitor before and after cutting/self-healing (inset of Fig.5D and 7D).The Rs of supercapacitor was about 3.1Ω, 3.6Ω, 3.9Ω, 4.2Ω, and 5.3Ω, corresponding to 0, 1th, 2th, 3th, 4th and 5th cutting/self-healing, respectively. And the Rct was 3.5Ω, 4.0Ω, 4.2Ω, 4.5Ω, and 5.5Ω, corresponding to 0, 1th, 2th, 3th, 4th and 5th cutting/self-healing, respectively. These results indicated that the resistance of the electrolyte and the charge transfer resistance of present supercapacitor slightly increased with increasing in cutting/self-healing cycles.The increasing in Rs may be attributed to that PANI/CC electrode was cut off. [40, 43, 46, 48]. The result also strongly confirmed the excellent self-healing performance for the present supercapacitor.

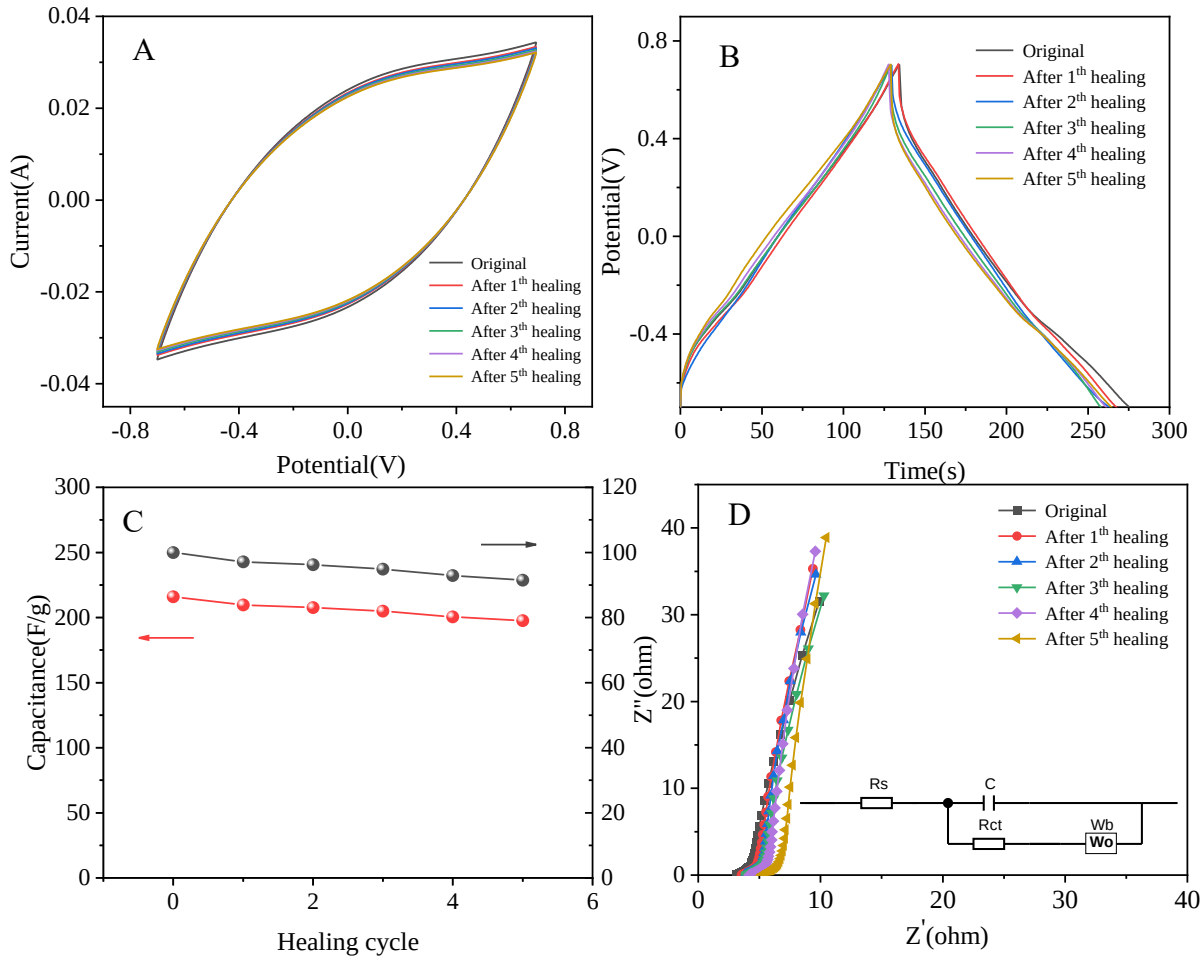

Fig.7. (A) CV curves and (B) GCD curves of supercapacitor based on

graphene/BA/PVA organo-hydrogel as a function of cutting/self-healing cycles. (C) (a) special capacitance and (b) capacitance retention, (D) EIS spectra of supercapacitor based on graphene/BA/PVA organo-hydrogel as a function of cutting/self-healing cycles. The inset of Fig.7D is Equivalent circuit model of present supercapacitor after cutting/self-healing.

The mechanical stability and flexibility of supercapacitor based on graphene/BA/PVA organo-hydrogel were also evaluated by the electrochemical performance as shown in Fig.8A-B. After multiple-time folds, the CV and GCD curves of the supercapacitor were few changes. It showed similar specific capacitance of 215 F/g, 221.4 F/g, 223.9 F/g and 211.0 F/g for bending angles of 0^o, 60^o, 90^o and 180^o, respectively (Fig.8B). In order to further verify the practical applications of the flexible supercapacitor, the output voltage of the supercapacitor was achieved by connecting three devices in series. By connecting 3 supercapacitors in series, the output voltage of 2.1V was obtained as shown in Fig.8(C-D). The supercapacitor was used as a power supply unit to light up a red LED (Fig.8E-F). As expected, LED light could both light up normally before and after cutting/self-healing. These results directly demonstrated the successful preparation of supercapacitor based on graphene/BA/PVA organo-hydrogel with excellent self-healing performance.

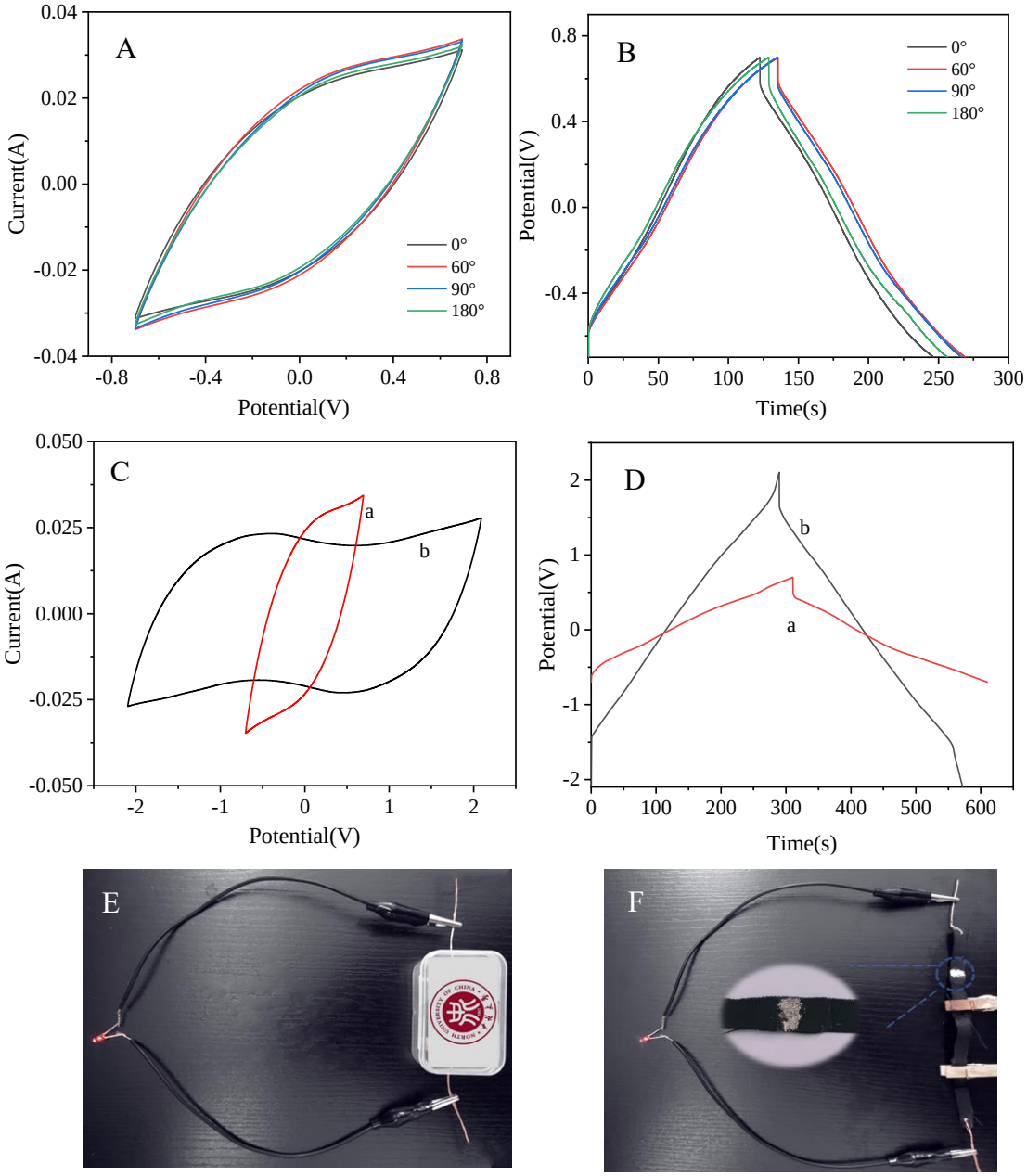

Fig.8. (A) CV curves and (B) GCD curves of supercapacitor based on graphene/BA/PVA organo-hydrogel under different bending angles. (C) CV curves and (D) GCD curve of three supercapacitor devices connected in series at 25℃. Optical photograph of a supercapacitor used as a red light-emitting diode power unit (E) before and (F) after cutting/self-healing.

4.Conclusion

In summary, a novel ternary network graphene/BA/PVA organo-hydrogel electrolyte was developed for application in supercapacitor with wide temperature adaptability and good self-healing properties. We obtained stable supercapacitor with specific capacitance of 215F/g at 2.0A/g at room temperature, which was improved and

reduced to 235.8F/g and 150.8F/g at 65℃ and -65℃, respectively. Furthermore, the supercapacitor also exhibited good self-healing performance, in which the capacitance retention of supercapacitor was about 90% after 5 cutting/self-healing cycles. These results confirmed the successful preparation of self-healing and wide temperature tolerant flexible supercapacitor based on ternary-network organo-hydrogel electrolyte for various applications.

Acknowledgments

Financial support from Shanxi Provincial Natural Science Foundation (202104021301059, 201803D421081, 201903D321045) and National Natural Science Foundation of China (U1810114).

Conflict of interest

The authors declared that they have no conflicts of interest to this work.

References

[1] Chen C R, Qin H, Cong H P, Yu S H. A Highly Stretchable and Real-Time Healable Supercapacitor [J]. Adv Mater, 2019, 31(19): e1900573.

[2] Liu Z, Liang G, Zhan Y, Li H, Wang Z, Ma L, Wang Y, Niu X, Zhi C. A soft yet device-level dynamically super-tough supercapacitor enabled by an energy-dissipative dual-crosslinked hydrogel electrolyte [J]. Nano Energy, 2019, 58(29): 732-742.

[3] Hassan M, Abbas G, Lu Y, Wang Z, Peng Z. A smart flexible supercapacitor enabled by a transparent electrochromic electrode composed of W18O49 nanowires/rGO composite films [J]. Journal of Materials Chemistry A, 2022, 10(9): 4870-4880.

[4] Peng H, Gao X, Sun K, Xie X, Ma G, Zhou X, Lei Z. Physically cross-linked dual-network hydrogel electrolyte with high self-healing behavior and mechanical strength for wide-temperature tolerant flexible supercapacitor [J]. Chemical Engineering Journal, 2021, 422(10): 130353-130360.

[5] Cheng Y, Xiao X, Pan K, Pang H. Development and application of self-healing materials in smart batteries and supercapacitors [J]. Chemical Engineering Journal, 2020, 380(16): 122565-122589.

[6] Guo M, Geng W C, Liu C B, Gu J Y, Zhang Z Z, Tang Y H. Ultrahigh Areal Capacitance of Flexible MXene Electrodes: Electrostatic and Steric Effects of

Terminations [J]. Chemistry of Materials, 2020, 32(19): 8257-8265.

[7] Li X, Lou D, Wang H, Sun X, Li J, Liu Y N. Flexible Supercapacitor Based on Organohydrogel Electrolyte with Long-Term Anti-Freezing and Anti-Drying Property [J]. Advanced Functional Materials, 2020, 30(52): 2007291-2007302.

[8] Liu C Y, Wang L, Xia Z P, Chen R X, Wang H L, Liu Y. Carbon hollow fibers with tunable hierarchical structure as self-standing supercapacitor electrode [J]. Chemical Engineering Journal, 2022, 431(2): 134009-134019.

[9] Hu Q, Shi X, Sun K, Cui S, Hamouda H A, Zhang W, Peng H, Ma G. A super-stretchable and thermally stable hydrogel electrolyte for high performance supercapacitor with wide operation temperature [J]. Journal of Alloys and Compounds, 2022, 909(4): 164646-164654.

[10] Liu J, Khanam Z, Ahmed S, Wang H, Wang T, Song S. A study of low-temperature solid-state supercapacitors based on Al-ion conducting polymer electrolyte and graphene electrodes [J]. Journal of Power Sources, 2021, 488(1): 229461-229473.

[11] Liu Q, Zhao A, He X, Li Q, Sun J, Lei Z, Liu Z H. Full-Temperature All-Solid-State Ti3C2Tx/Aramid Fiber Supercapacitor with Optimal Balance of Capacitive Performance and Flexibility [J]. Advanced Functional Materials, 2021, 31(22): 2010944-2010955.

[12] Liu Y, Li H, Wang X, Lv T, Dong K, Chen Z, Yang Y, Cao S, Chen T. Flexible supercapacitors with high capacitance retention at temperatures from −20 to 100 °C based on DMSO-doped polymer hydrogel electrolytes [J]. Journal of Materials Chemistry A, 2021, 9(20): 12051-12059.

[13] Lu C, Chen X. All-Temperature Flexible Supercapacitors Enabled by Antifreezing and Thermally Stable Hydrogel Electrolyte [J]. Nano Lett, 2020, 20(3): 1907-1914.

[14] Xu J, Jin R, Ren X, Gao G. A wide temperature-tolerant hydrogel electrolyte mediated by phosphoric acid towards flexible supercapacitors [J]. Chemical Engineering Journal, 2021, 413(10): 127446-127453.

[15] Yang G, Huang J, Wan X, Zhu Y, Liu B, Wang J, Hiralal P, Fontaine O, Guo Y, Zhou H. A low cost, wide temperature range, and high energy density flexible quasi-solid-state zinc-ion hybrid supercapacitors enabled by sustainable cathode and

electrolyte design [J]. Nano Energy, 2021, 90(9): 106500-106510.

[16] Yang Y, Wang K-P, Zang Q, Shi Q, Wang Y, Xiao Z, Zhang Q, Wang L. Anionic organo-hydrogel electrolyte with enhanced ionic conductivity and balanced mechanical properties for flexible supercapacitors [J]. Journal of Materials Chemistry A, 2022, 10(20): 11277-11287.

[17] Ye L, Liang Q, Huang Z-H, Lei Y, Zhan C, Bai Y, Li H, Kang F, Yang Q-H. A supercapacitor constructed with a partially graphitized porous carbon and its performance over a wide working temperature range [J]. Journal of Materials Chemistry A, 2015, 3(37): 18860-18866.

[18] Zhong M, Tang Q F, Qiu Z G, Wang W P, Chen X Y, Zhang Z J. A novel electrolyte of ternary deep eutectic solvent for wide temperature region supercapacitor with superior performance [J]. Journal of Energy Storage, 2020, 32(18): 101904-101914.

[19] Li H, Lv T, Li N, Yao Y, Liu K, Chen T. Ultraflexible and tailorable all-solid-state supercapacitors using polyacrylamide-based hydrogel electrolyte with high ionic conductivity [J]. Nanoscale, 2017, 9(46): 18474-18481.

[20] Fan X, Liu J, Song Z, Han X, Deng Y, Zhong C, Hu W. Porous nanocomposite gel polymer electrolyte with high ionic conductivity and superior electrolyte retention capability for long-cycle-life flexible zinc–air batteries [J]. Nano Energy, 2019, 56(22): 454-462.

[21] Wang S B, Zhang D, He X M, Yuan J F, Que W B, Yang Y R, Protsak I, Huang X X, Zhang C, Lu T X, Pal P, Liu S Q, Zheng S Y, Yang J T. Polyzwitterionic double-network ionogel electrolytes for supercapacitors with cryogenic-effective stability [J]. Chemical Engineering Journal, 2022, 438(3): 135607-135615.

[22] Han X Y, Li J, Lu J L, Luo S, Wan J, Li B X, Hu C G, Cheng X L. High mass-loading NiCo-LDH nanosheet arrays grown on carbon cloth by electrodeposition for excellent electrochemical energy storage [J]. Nano Energy, 2021, 86(4): 106079-106088.

[23] Liu T, Li C Y, Liu H C, Zhang S, Yang J L, Zhou J, Yu J L, Ji M W, Zhu C Z, Xu J. Tear resistant Tyvek/Ag/poly(3,4-ethylenedioxythiophene): Polystyrene sulfonate (PEDOT:PSS)/carbon nanotubes electrodes for flexible high-performance

supercapacitors [J]. Chemical Engineering Journal, 2021, 420(12): 127665-127674.
[24] Yu Y, Xu A Z, Zhang Y, Li W, Qin Y J. Evaporation-induced hydrated graphene/polyaniline/carbon cloth integration towards high mass loading supercapacitor electrodes [J]. Chemical Engineering Journal, 2022, 445(4): 136727-136736.
[25] Ye Y, Zhang Y, Chen Y, Han X, Jiang F. Cellulose Nanofibrils Enhanced, Strong, Stretchable, Freezing-Tolerant Ionic Conductive Organohydrogel for Multi-Functional Sensors [J]. Advanced Functional Materials, 2020, 30(35): 2003430-2003441.
[26] Lin Y X, Zhang H Y, Liao H Y, Zhao Y, Li K. A physically crosslinked, self-healing hydrogel electrolyte for nano-wire PANI flexible supercapacitors [J]. Chemical Engineering Journal, 2019, 367(2): 139-148.
[27] Qiu M N, Zhang S K, Abbas Y, Zhang C Y, Liu W, Wu Z P, Dai S T, Zhang T. Heteroatom-doped ultrahigh specific area carbons from hybrid polymers with promising capacitive performance [J]. Journal of Power Sources, 2020, 478(16): 228761-228774.
[28] Qin L, Yang G, Li D, Ou K, Zheng H, Fu Q, Sun Y. High area energy density of all-solid-state supercapacitor based on double-network hydrogel with high content of graphene/PANI fiber [J]. Chemical Engineering Journal, 2022, 430(11): 133045-133054.
[29] Peng H, Lv Y, Wei G, Zhou J, Gao X, Sun K, Ma G, Lei Z. A flexible and self-healing hydrogel electrolyte for smart supercapacitor [J]. Journal of Power Sources, 2019, 431(10): 210-219.
[30] Joo H, Han H, Cho S. Fabrication of Poly(vinyl alcohol)-Polyaniline Nanofiber/Graphene Hydrogel for High-Performance Coin Cell Supercapacitor [J]. Polymers (Basel), 2020, 12(4): 928-943.
[31] Guo G, Sun Y, Fu Q, Ma Y, Zhou Y, Xiong Z, Liu Y. Sol-gel synthesis of ternary conducting polymer hydrogel for application in all-solid-state flexible supercapacitor [J]. International Journal of Hydrogen Energy, 2019, 44(12): 6103-6115.
[32] Zheng H, Guan R, Liu Q, Ou K, Li D-s, Fang J, Fu Q, Sun Y. A flexible supercapacitor with high capacitance retention at an ultra-low temperature of -65.0°C

[J]. Electrochimica Acta, 2022, 424(10): 140644-140655.

[33] Li Z W, Chen D H, An Y F, Chen C L, Wu L Y, Chen Z J, Sun Y, Zhang X G. Flexible and anti-freezing quasi-solid-state zinc ion hybrid supercapacitors based on pencil shavings derived porous carbon [J]. Energy Storage Materials, 2020, 28(14): 307-314.

[34] Liu Z, Zhang J, Liu J, Long Y, Fang L, Wang Q, Liu T. Highly compressible and superior low temperature tolerant supercapacitors based on dual chemically crosslinked PVA hydrogel electrolytes [J]. Journal of Materials Chemistry A, 2020, 8(13): 6219-6228.

[35] Lu N, Na R Q, Li L B, Zhang C Y, Chen Z Q, Zhang S L, Luan J S, Wang G B. Rational Design of Antifreezing Organohydrogel Electrolytes for Flexible Supercapacitors [J]. Acs Applied Energy Materials, 2020, 3(2): 1944-1951.

[36] Ren Y Y, Guo J N, Liu Z Y, Sun Z, Wu Y Q, Liu L L, Yang F. Ionic liquid-based click-ionogels [J]. Science Advances, 2019, 5(8): 648-657.

[37] Rong Q, Lei W, Huang J, Liu M. Low Temperature Tolerant Organohydrogel Electrolytes for Flexible Solid-State Supercapacitors [J]. Advanced Energy Materials, 2018, 8(31): 1801967-1801973.

[38] Tong R P, Chen G X, Pan D H, Qi H S, Li R A, Tian J F, Lu F C, He M H. Highly Stretchable and Compressible Cellulose Ionic Hydrogels for Flexible Strain Sensors [J]. Biomacromolecules, 2019, 20(5): 2096-2104.

[39] Zhi H, Fei X, Tian J, Jing M Z, Xu L Q, Wang X Y, Liu D M, Wang Y, Liu J Y. A novel transparent luminous hydrogel with self-healing property [J]. Journal of Materials Chemistry B, 2017, 5(29): 5738-5744.

[40] Dai L-x, Zhang W, Sun L, Wang X-h, Jiang W, Zhu Z-w, Zhang H-b, Yang C-c, Tang J. Highly Stretchable and Compressible Self-Healing P(AA-co -AAm)/CoCl2

Hydrogel Electrolyte for Flexible Supercapacitors [J]. ChemElectroChem, 2019, 6(2): 467-472.

[41] Guo Y, Zheng K, Wan P. A Flexible Stretchable Hydrogel Electrolyte for Healable All-in-One Configured Supercapacitors [J]. Small, 2018, 14(14): e1704497-e1704505.

[42] Huang H, Han L, Fu X, Wang Y, Yang Z, Pan L, Xu M. A Powder Self-Healable Hydrogel Electrolyte for Flexible Hybrid Supercapacitors with High Energy Density and Sustainability [J]. Small, 2021, 17(10): e2006807-e2006816.

[43] Huang Y, Zhong M, Huang Y, Zhu M, Pei Z, Wang Z, Xue Q, Xie X, Zhi C. A self-healable and highly stretchable supercapacitor based on a dual crosslinked polyelectrolyte [J]. Nat Commun, 2015, 6(9): 10310-10319.

[44] Ma W-B, Zhu K-H, Ye S-F, Wang Y, Guo L, Tao X-Y, Guo L-T, Fan H-L, Liu Z-S, Zhu Y-B, Wei X-Y. A self-healing hydrogel electrolyte towards all-in-one flexible supercapacitors [J]. Journal of Materials Science: Materials in Electronics, 2021, 32(15): 20445-20460.

[45] Wei D, Wang H, Zhu J, Luo L, Huang H, Li L, Yu X. Highly Stretchable, Fast Self-Healing, Responsive Conductive Hydrogels for Supercapacitor Electrode and Motion Sensor [J]. Macromolecular Materials and Engineering, 2020, 305(5): 2000018-2000029.

[46] Siyahjani S, Oner S, Diker H, Gultekin B, Varlikli C. Enhanced capacitive behaviour of graphene based electrochemical double layer capacitors by etheric substitution on ionic liquids [J]. Journal of Power Sources, 2020, 467(10): 228353-228361.

[47] Obeidat A M, Luthra V, Rastogi A C. Solid-state graphene-based supercapacitor with high-density energy storage using ionic liquid gel electrolyte: electrochemical properties and performance in storing solar electricity [J]. Journal of Solid State Electrochemistry, 2019, 23(6): 1667-1683.

[48] Kim M S, Kim J W, Yun J, Jeong Y R, Jin S W, Lee G, Lee H, Kim D S, Keum K, Ha J S. A rationally designed flexible self-healing system with a high performance supercapacitor for powering an integrated multifunctional sensor [J]. Applied Surface Science, 2020, 515(6): 146018-146028.